

UNCLASSIFIED

Defense Technical Information Center
Compilation Part Notice

ADP011350

TITLE: Design and Production of Color Calibration Targets for Digital Input Devices

DISTRIBUTION: Approved for public release, distribution unlimited

This paper is part of the following report:

TITLE: Input/Output and Imaging Technologies II. Taipei, Taiwan, 26-27 July 2000

To order the complete compilation report, use: ADA398459

The component part is provided here to allow users access to individually authored sections of proceedings, annals, symposia, etc. However, the component should be considered within the context of the overall compilation report and not as a stand-alone technical report.

The following component part numbers comprise the compilation report:

ADP011333 thru ADP011362

UNCLASSIFIED

Design and production of color calibration targets for digital input devices

Chao-hua Wen and Jyh-jiun Lee

Opto-Electronics & Systems Laboratories, Industrial Technology Research Institute
Hsin-chu, Taiwan, ROC

ABSTRACT

This paper presents the design and production of calibration targets for digital input color devices. By experimentally determined gamut of surface color, this study redesigns the aim values based on ISO/FDIS 12641 and to meet process specifications of Noritsu QSS23-HRCRT photographic printer with silver halide photography. The calibration target includes four components: a set of 144 color patches (3 levels in lightness and 4 levels in chroma at 12 different hue angles) within printing gamut, a neutral scale containing 22 steps based on visual perception, a set of C-M-Y-K-R-G-B dye scales showing characteristics of photographic materials, and a series of facial colors ranked by red. This research will describe the meaning of each element, the use of colorimetric mapping to CIELCH for each element, the conversion of these patch into a RGB-mode electronic image file, and how to control the processing of color photographic materials. And we propose an approach of dynamic subgroup linear interpolation to achieve high process quality of manufacturing calibration targets and cost-down. Finally, statistic results revealed that 99% of the patches are within 10 delta Eab of the aim values specified in this study from long-term test and 99% of the patches in the manufacturing batch are within 5 delta Eab of the mean values from short-term test.

Keywords: Calibration target, Test chart, Color gamut, Process control

1. INTRODUCTION

While color digital input devices are now used to capture images for output on a variety of media, their development has essentially taken place within a Graphic Arts environment. Digital input devices have the same problem that is the task of making a colored image in a reproduction "match" a colored image in the original under some specified illuminant in Graphic Arts. The most efficient method for characterizing a scanner or digital camera is to image a set of aimed colors of known tristimulus values.¹ Using color calibration techniques, the data obtained from this imaging process can be compared to the tristimulus values of the test image and a colour transformation defined.

A range of tools has been developed by ANSI, consisting of a series of photographic prints and transparencies, which are used for characterizing an input scanner. The specifications are now being circulated by ISO as ISO 12641.² A color test image has been designed based on the Kodak Q60TM test transparency described by Maier and Rinehart,³ and this image has been made on a range of materials from each of the major film suppliers. Kodak supplies the image on both Kodachrome and Ektachrome transparency material, and Fuji and Agfa supply it on Fujichrome and Agfachrome respectively. Each of the vendors also supplies the same image on their print materials. (Konica is also heavily involved in the development of this target but currently has no plan to market it.)

However, those expensive products result in low usability for end users, "calibrated" targets especially. The reasons are as follows. First, ISO 12641 is strict with the chroma values, which are not easily achieved by other manufacturers beyond above four vendors. Significantly, the colorimetric aim values of the target are designed around the characteristics of color transparency film and photographic paper. For example, manufacturers shall test the maximum chroma at each defined lightness and hue, if they use different photographic materials. Second, the traditional manufacturing approach is very time-consuming during making the intermediate film. Third, the techniques for process control in producing targets are expertise and the requirements for achieving satisfactory control are rigorous. Final, it is originally intended that vendor would

Correspondence: Chao-hua Wen; OES/ITRI, S010, B51, 195-8, Sec. 4, Chung-Hsing Rd., Chu-tung, Hsin-chu 310, Taiwan, R.O.C.; Email: h880021@itri.org.tw; Telephone: 886-3-5913714; Fax: 886-3-5829781.

provide the "calibrated" target so that the user could know the tristimulus values of each patch on that specific target. This would be necessary for those who require device independent calibrations and have no appropriate color measuring facilities themselves. However, early experiences suggested that, for some vendors at least, the sample variation within a batch was sufficiently small that use of a batch calibration data set was adequate for all but the most critical users. For this reason, at least one of the vendors (Kodak) has chosen to make batch average data for their targets available from an Internet site: <ftp://ftp.kodak.com/gastds/Q60DATA/>.

To overcome these barriers, this study proposes a new approach of calibration target design and manufacture. First, we discuss with the requirements of the calibration target. Second, this article describes how to design the calibration target that differs from Maier and Rinehart³ and specifies how to modify the aim values of the ISO/FDIS 12641 color patches for meeting process capability of color reproduction. Third, we draw the processes of conversion of numerical CIELCH data for each patch into a sRGB-mode electronic image file. Fourth, this study explains how to use dynamic subgroup linear interpolation (DSL_I) and statistic process control (SPC) to achieve high process quality of printing calibration targets and cost-down. Finally, a brief of discussion and conclusions has been made for future researches.

2. REQUIREMENTS OF THE CALIBRATION TARGET

This research primarily addresses itself on the reflection target. IT8.7/2-1993 consists of a series of single dye scales (cyan, magenta and yellow) with equivalent two- and three-dye combinations.⁴ These scales are particularly useful in setting up many scanners since the resultant colors are similar to the regions of color space in which the scanners permit independent. The remaining colors consist of 12 samples at each of 12 hues. The samples include four chroma levels at each of three lightness levels. Each of the lightness intervals and each of chroma intervals are approximately equally spaced, and each of maximum chroma which material can be achieved is produced at each lightness and hue level. A 22 step gray scale is also included. Apart from above specific values, the target also contains the D_{min} and D_{max} and 36 vendor selected colors. Therefore, IT8.7/2-1993 provides altogether 288 colors.

Thus, the calibrated color target provides known tristimulus values which cover, more or less uniformly, the full colour gamut of the specific material on which the target has been imaged, as an input to the color scanner characterization. In one word, the target must have a set of colored patches that cover the color gamut of the photographic material and important and common hues. The colored patches could also provide a guide for making the color correction adjustments on the electronic color separation scanner and an orderly pattern to facilitate automated evaluation of predetermined values stored in a look-up table. Kang also concluded that the position of the color used for training is more important in the color interpolation within a given gamut rather than the number of colors.⁵

3. DESIGN AND SPECIFICATION OF THE CALIBRATION TARGET

Figure 1 demonstrates the architecture of calibration target design and production, as follows. First, the best printing and processing conditions will be determined via the experimental design. Second, color gamuts will be illustrated for understanding the limitation of color reproduction by a field study, not by computing methods⁶⁻⁷. Third, the color values of target have been specified that according to experimental color gamuts. Fourth, color transform from CIELCH to sRGB will be described. Fifth, the relevant target mockups will be created. Sixth, the quality will be controlled by SPC during daily setup. Seventh, the method of DSL_I will be adopted to refine the electronic target mockup. Final, an experiment will show how to supervise the quality of photographic printer and processor for meeting the aim values. This chapter focuses on preparatory works, color theories, calibration target design and specification of the targets from the first stage to the fifth stage. The remainders will be discussed on the next chapter.

This study applies the CIE 1976 ($L^*a^*b^*$) color space or the CIELAB color space to design the color calibration target.⁸ Uniform spacing in hue, lightness and chroma, and tolerance in terms of differences in these parameters (ΔE_{ab}) is believed to provide a reasonable distribution of target patches in the most effective manner. In this color space, L^* represents lightness and a^*-b^* coordinates indicate the hue and chroma information. Hewlett-Packard and Microsoft proposed the addition of support for a standard color space, sRGB, within the Microsoft operating systems, HP products, the Internet, and all other interested vendors. The aim of this color space is to complement the current color management strategies, particularly ICC, by enabling a simple method of handling color in operating systems and the WWW.⁹ This method utilizes a simple and robust color space definition that will be applied.

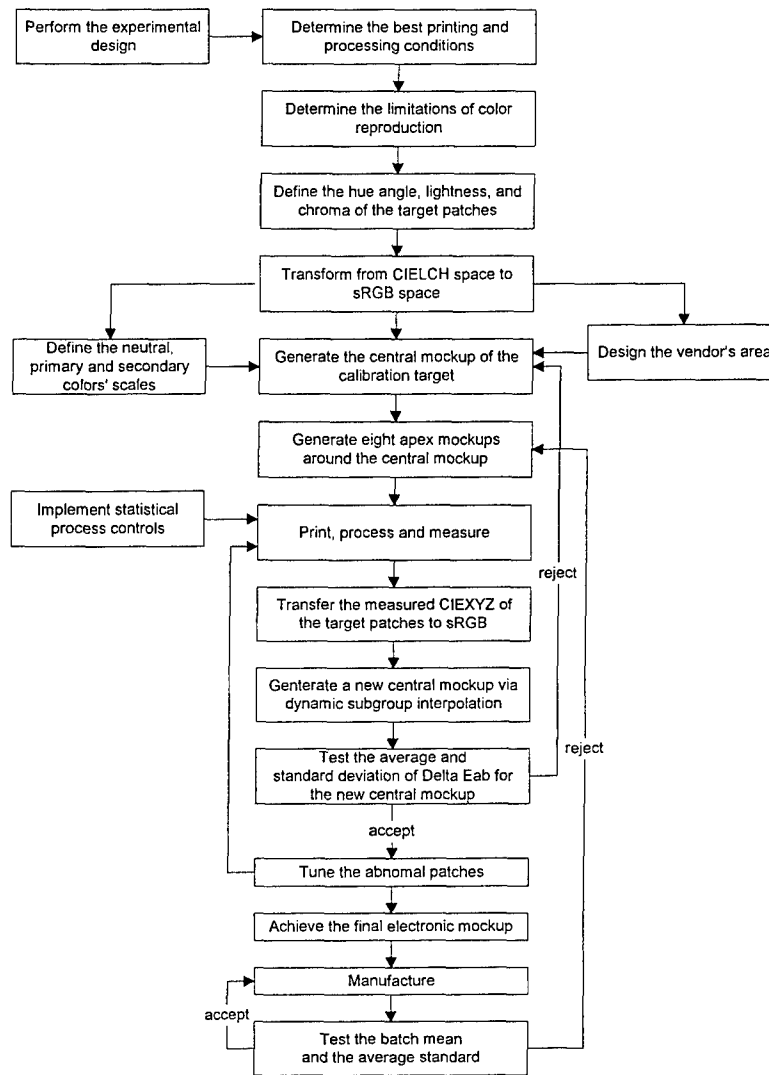


Figure 1. The architecture of calibration target design and production

3.1. Determination of printing and processing conditions

Today's photographic market is rapidly changing. This is primarily due to internal developments and growing influence of external factors. These factors are attribute to digital electronics, communications, entertainment and leisure-time opportunities. Efforts to render digital images onto silver-halide paper and film for commercial are quite recent.

Recently, Noritsu's QSS23-HRCRT with the high resolution CRT printer has become available in the market. HRCRT is short for Hyper Resolution Cathode Ray Tube. This is a digital printing engine with higher quality of 500 or 300 dpi prints in minilab industry and suitable for high-end users. We use 500 dpi for high performance of the HRCRT in this study. The HRCRT electron beam lights up three phosphor lines: blue, green, and red. The paper is then pressed against the HRCRT tube faceplate (without any lens) and exposed. The processing capacity of HRCRT printer is 122 prints per hour for size of 127mm (width) \times 178mm (advance length) under 500dpi.

We use Kodak Professional Digital Paper Type 2976 that is designed for digital printers rather than Royal series paper that is designed for optical exposure. Moreover, we use Kodak Ektacolor RA chemical for Process RA-4 to process the digital paper under normal replenishment rate. In addition, gamma of the HRCRT plug-in driver has been tested and settled on 1.8 by way of printing gray scale at varied gamma levels.

3.2. Color gamut of color reproduction

Figure 2 represents the color gamuts of Kodak digital paper type 2976, Kodak Royal VII paper and sRGB. This plot shows all points on the a^*-b^* plane without information about the L^* . The sRGB's color gamut is obtained from calculating all points of RGB $32 \times 32 \times 32$, and color gamuts of two kinds of paper are measured from printing all points of RGB $17 \times 17 \times 17$ respectively. The orange enclosure is the gamut of Kodak professional digital paper type 2976. The black enclosure is the gamut of Kodak Royal 7 Color paper. And the blue one is the gamut of sRGB. Figure 2 also shows that the gamut of sRGB is wider than papers.

One phenomenon is worthy to be mentioned that papers give larger gamuts in yellow and cyan colors than sRGB. Unfortunately, Figure 2 reveals accurate hue information, but without the lightness information. The plot of L^*-C^* provides a suitable second graph, as show in Figure 3, to represent CIELAB color space. Although this plot contains only colors at the specified hue angle, this diagram is most useful for depicting the color gamut of a system at a particular hue angle. Figure 3 also demonstrates that some specified colors in IT8.7/2-1993 are outside of color gamut of digital paper after printing and processing, such as F3, G3, H3, and L3. With these color gamuts, this research can now define color patches for the calibration target and that will be discussed in the next section.

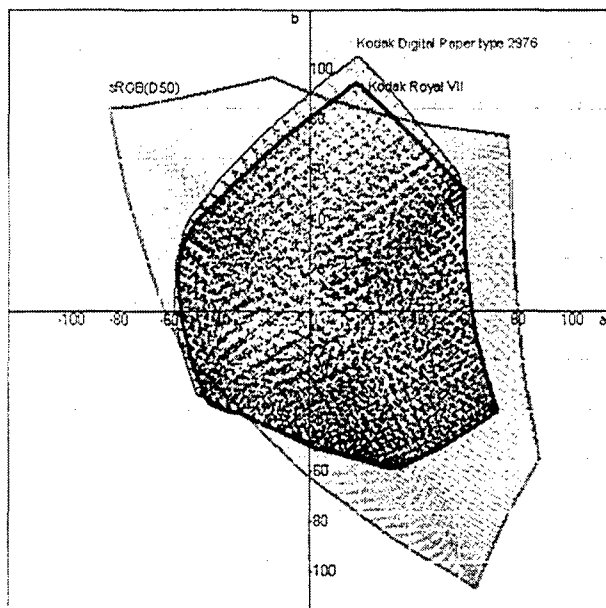


Figure 2. Comparisons of color gamuts among Kodak digital paper type 2976, Kodak Royal VII paper and sRGB

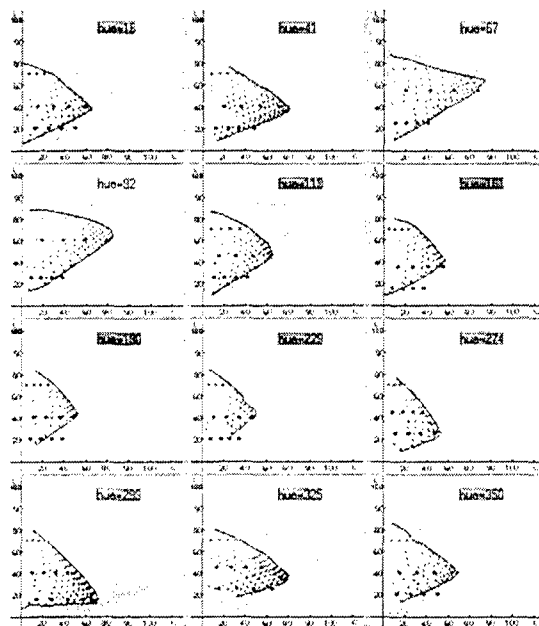


Figure 3. L^*-C^* Diagrams showing the gamuts of digital paper (dark) and sRGB (light) for 12 hue angles (the block points are aim values specified in IT8.7/2-1993)

3.3. Specification of target patches

Good color photography is expected to achieve large color gamuts and stable neutral grays. However there is a general tendency that three dyes giving large color gamuts give unstable neutral grays. Modern color photography tends to adopt the three dyes giving large color gamuts at the expense of the stable neutral grays. Therefore, the first thing is to define the neutral scale. Anyway, we follow the definition of neutral scale in IT8.7/2-1993. The neutral scale has equal visual intervals, which in CIELAB color space means equal interval in L^* . The range in densities is from white to black. For this scale to be neutral, $a^* = 0$ and $b^* = 0$. This study also complies with the specifications of the primary color, the secondary color and black scales in ISO 12641.

In accordance with results of section 3.2, this paper modifies parts of the definition of IT8.7/2-1993 about color gamut mapping. We retained the hue information as well as IT8.7/2-1993. This research also kept the L^* value that is defined in IT8.7/2-1993 as far as possible. Additionally, this study performs in conformity with the essence of chroma specification in IT8.7/2-1993, which is equal space in chroma. All color gamut-mapping patches are listed in Table 1.

A "vendor-optional" area is provided so that different target manufacturer can add unique elements by self-determination. Here, we investigate the facial colors of Kodak Q60 color input target, Fuji color target and real humankind in CIELAB color space, as shown in Figure 4. Diamonds represent the 20 column patches of Fuji color target, squares denote the 21 column patches of Fuji color target, triangles show the 22 column patches of Fuji color target. Circles mean 12 patches from L20 to L22 of Kodak Q60 color input target. And asterisks indicate skin colors (forehead/cheek) of African, Arabian, Caucasian, Japanese and Vietnamese respectively. Fortunately, sorting those colors by red after transforming facial colors form CIELAB to sRGB (discussed in next section) that clue us in facial color self-determination, depicted in Figure 5. Diamond denotes red, square denotes green and triangle denotes blue. Two arrows point out the two outliers in blue channel. The reason of sorting by red channel is that people's blood is hot red. And Figure 5 evidences this hypothesis. Red is rapidly increased between 0 and 150 and is convergent between 200 and 220. Generally, blue have the same trend as green and blue is smaller than green. Next, we used polynomial curve fitting to find the coefficients of three appropriate polynomials that fit the R, G and B data individually. Finally, we calculate the values of the polynomials evaluated at equal intervals that are equal divided the number of effective sampling facial colors into the number of demanded patches.

Table 1. Hue angle, lightness and chroma

| Row | Hue Angle | L1 | L2 | | | | L3 | L4 | | | |
|-----|-----------|-----|-----|-----|-----|-----|----|-----|-----|-----|-----|
| | | | C1 | C2 | C3 | C4 | | C1 | C2 | C3 | C4 |
| A | 16 | 20 | 9* | 18* | 27* | 36* | 40 | 15 | 30 | 44 | 62* |
| B | 41 | 20 | 10* | 20* | 30* | 40* | 40 | 20 | 36 | 54 | 76* |
| C | 67 | 25 | 9* | 18* | 27* | 36* | 55 | 22 | 44 | 66 | 81* |
| D | 92 | 25 | 7* | 14* | 21* | 28* | 60 | 20 | 40 | 60 | 80* |
| E | 119 | 25 | 8* | 16* | 24* | 33* | 45 | 14* | 28* | 42* | 56* |
| F | 161 | 20* | 6* | 12* | 18* | 25* | 35 | 11* | 22* | 33* | 43* |
| G | 190 | 20 | 6* | 12* | 18* | 23* | 40 | 13 | 25 | 38 | 49* |
| H | 229 | 20 | 6* | 12* | 18* | 23* | 40 | 12 | 24 | 36 | 45* |
| I | 274 | 25 | 12* | 24* | 36* | 48* | 45 | 9 | 19 | 28 | 35* |
| J | 299 | 15 | 14* | 28* | 42* | 56* | 40 | 11 | 22 | 33 | 51* |
| K | 325 | 25 | 14* | 28* | 42* | 56* | 45 | 14 | 28 | 42 | 70* |
| L | 350 | 20 | 9* | 18* | 27* | 35* | 40 | 16 | 32 | 48 | 66* |

Asterisks denote modified or self-determined color patch values

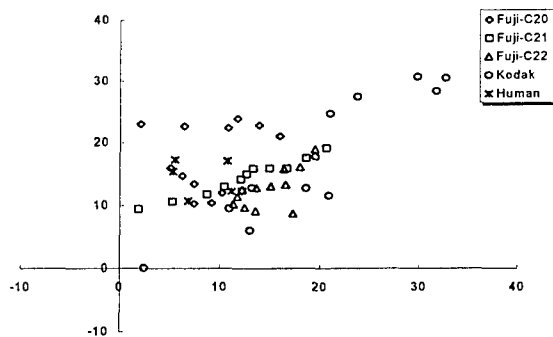


Figure 4. Collected facial colors in CIELAB color space.

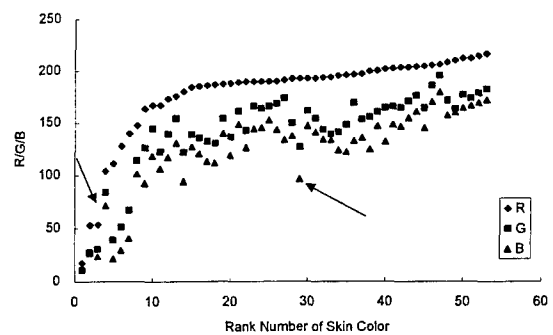


Figure 5. The appearance of facial colors, which are sorted by red after transforming CIELAB to sRGB

3.4. Generation of the electronic target mockup

The electronic target mockup is for digital printer. Because the QSS2301-HRCRT only receives the image file of 24-bit RGB color mode, transforming color spaces from CIELCH to sRGB at the D50 white point should be discussed firstly. In general, many publishers only write the calculation processes of color space transformation from XYZ to CIELCH. Since Stokes et al. proposed the sRGB color space,⁹ the sRGB has been widely introduced to the color management system. However, the D50 white point of the profile connection space is included in the header of the profile, but the white point is set to D65 of the sRGB monitor. Recently, Nielsen and Stokes proposed a 3x3 matrix transforming sRGB to XYZ at D50, which is the product of the reduced Bradford chromatic adaptation matrix and the sRGB matrix at D65, to clear up the confusion.¹⁰

This study developed a generator of the electronic semi-mockup for the calibration target. The generator had two main functions. One is that transforms the 288 patch color values from XYZ to sRGB, and makes up an initial/central semi-mockup which size is 416x288 pixels or produces an apex semi-mockup which is based on both of the setting interval and the central semi-mockup. The intention of apex semi-mockups prepared for DSLI will be described in next chapter. The other is that performs DSLI. Figure 6 shows the initial electronic semi-mockup image. This is not a finish mockup, but it is still necessary to edit the image file for meeting the specifications of QSS2301-HRCRT, such as image resolution, image size, labels of the calibration target, and so on. We used Photoshop 5.0 as a tool for editing the image file of semi-mockup to finish the electronic target mockup.

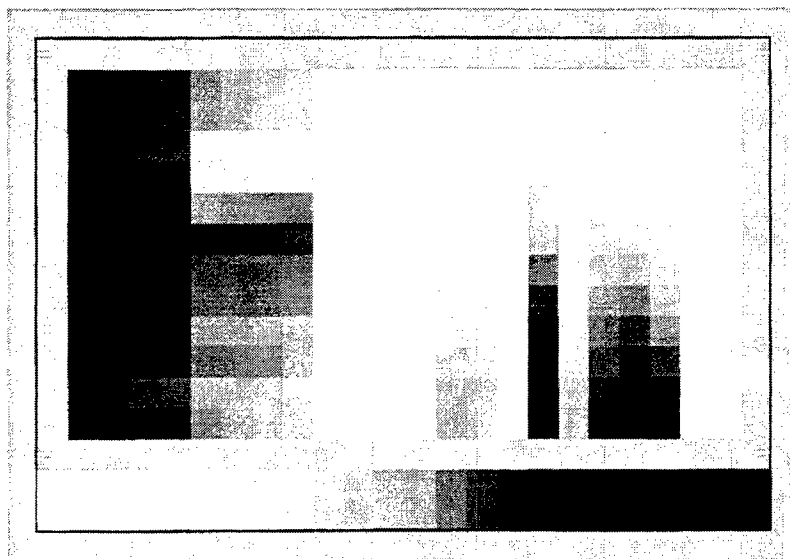


Figure 6. The initial electronic semi-mockup

4. QUALITY OF THE PRODUCTION PROCESS

Quality control in manufacturing the calibration target is a very important issue. ISO 12641 specifies that the "un-calibrated" target patches contained with A1 through L3, A5 through L7, and A9 through L11, 99% shall be within 10 delta Eab* of the aim values for all targets manufactured. ISO 12641 also specifies that 99% of the "un-calibrated" target patches within the manufacturing batch shall be within 5 delta Eab* of the reference for each manufacturing batch. The reference are reported batch means for patches A1 through L19, Dmin and Dmax, and the aim values specified in this standard for 22-step neutral scale.² However, those manufacturing tolerances have been set which are capable of being achieved over a significant number of targets and have been considered how to meet the objective of minimizing variations as far as reasonable. Following sections will discuss how to implement DSLI to refine a "gold" electronic target mockup and how to introduce SPC into supervising the printing and processing processes. Finally, experimental results demonstrated one general principle for controlling the calibration target manufacturing process.

4.1. Dynamic subgroup linear interpolation

Color space transitions are frequently used in image processing as mention in the previous chapter. A image encoded in a device-independent representation, such as CIELAB, CIELUV and XYZ, needs to be transformed to the device space of the monitor before it can be displayed and to the colorants of printer before it can be printed. Unfortunately, the interaction of light with the dyes and pigments of practical printers to form colors is more complex than the color-forming mechanisms of CRTs, making it more difficult to construct an accurate mathematical model for a printer.¹¹ It is possible to specify arbitrary transfer functions in terms of three-dimensional lookup tables, but the requirement of huge storage and the unpredictable quality of printing are shortcomings of this approach. Here, we propose DSLI to overcome above drawbacks.

The goal of this research is to produce accuracy 288 patches of the calibration target, not to improve image quality. After color space transforming from CIELCH to sRGB, we can acquire the results that are near but are not exact. Thus, those principles inspired the design concept of dynamic subgroup linear interpolation. The approach is not necessary to construct an accurate mathematical model for QSS23-HRCRT printer or build the huge-volume lookup table for high printing quality. But the approach creates one subgroup for each patch. The subgroup is called body-centered-cubic packing that consists of nine patches, one center and eight apices. This is shown in Figure 7. Intuitively, the initial electronic mockup consists of 288 patches can be conceive as a central mockup and can be used to generate the other eight apex mockups. The size of the subgroup depends on the magnitude of color difference between the central mockup and its aim values. Therefore, this paper simply stores the color values of 288 subspaces for the output function evaluated at discrete points in the input space.

Following printing and processing those nine electronic mockups with QSS2301-HRCRT, we measured them by Gretag Macbeth Spectrolino & SpectroScan. The color measurements were performed on a black backing in accordance with ISO 5/4 under the conditions 45/0 geometry, no polarization, no filter, 2° observer, D50, XYZ system. Next we transforms the measured XYZ values of nine mockups to sRGB space. The simple linear interpolation in one dimension is enough to evaluate the function between inputs and outputs in this study. The procedures are as follows: (1) calculate the individual RGB color difference between output and its aim value for each subgroup, (2) search the minimum of RGB difference and determine the direction of interpolation, and (3) evaluate the new value. Because the complex interaction of paper dyes, the algorithm should be noted when small value occurs.

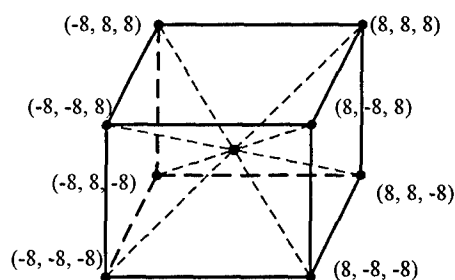


Figure 7. One example of body-centered-cubic packing

4.2. Supervision of photographic printer and processor

From a photographic profession's viewpoint, color balance is a fundamental requirement for getting the best quality of color reproduction. Observation the reproduction of the gray scale is frequently used in color balance. This study adopted the 18 step daily setup to control the exposure of QSS23-HRCRT. Although the function of daily setup is automatic that we cannot intervene, the process stability of daily setup is a critical factor that may supervise the quality of chemicals and archive the high output quality. We develop a method from the concept of SPC into monitoring the primary quality during research and design phase. However, we believe that the method is adequate to the manufacturing lineup.

During daily setup, Densities of 18 steps are measured by the inner densitometer of QSS23-HRCRT and are displayed in RGB. These raw data are miscellaneous. The most commonly used measure of location or tendency is the mean and two measures of dispersion extremely used are the range and the standard deviation.¹² For simplifying and characterizing, the measures are not classical statistic forms any more, but they still contain both basic and specific information. In this study, for each sample of 18 step density, the average and standard deviation (the reference is the overall mean density of each step, not the average) were computed for each channel. Two control charts had been drawn to monitor the materials, manufacturing processes, and so forth. Figure 8 and Figure 9 illustrate an X-bar chart for monitoring the location parameter

and an S (standard deviation) chart for monitoring the dispersion parameter respectively. From the past experience, one time of daily setup is not enough to steady the printing and processing of QSS23-HRCRT. This results in a varied of sampling sizes for one test. In general, performing three to eight times daily setup are necessary for good quality, shown in Figure 9. The first time of daily setup has the largest standard deviation. However, continual daily setups could help decrease the standard deviation. Finally, results revealed that we should control the standard deviation below its average as far as possible.

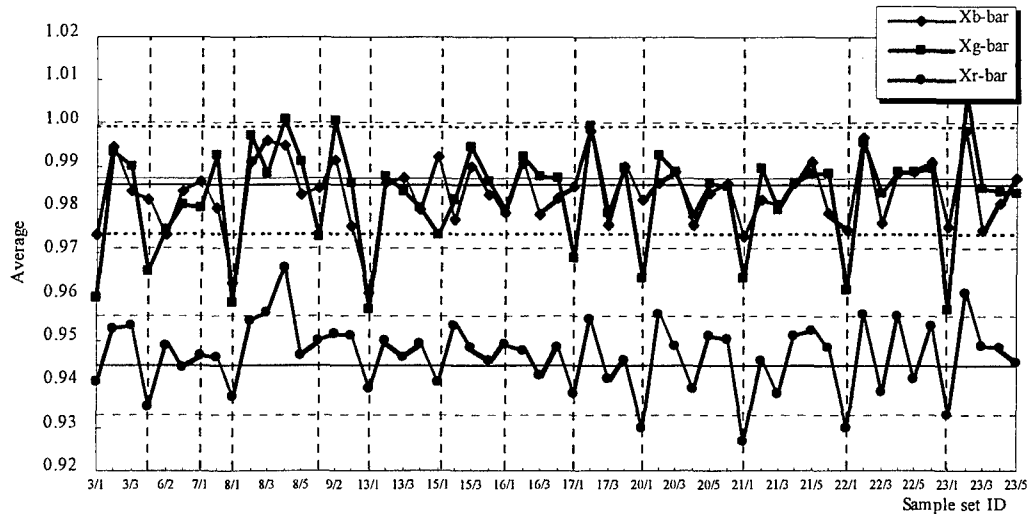


Figure 8. Control chart for averages, X-bars, with 3-sigma control limits for 13 running days

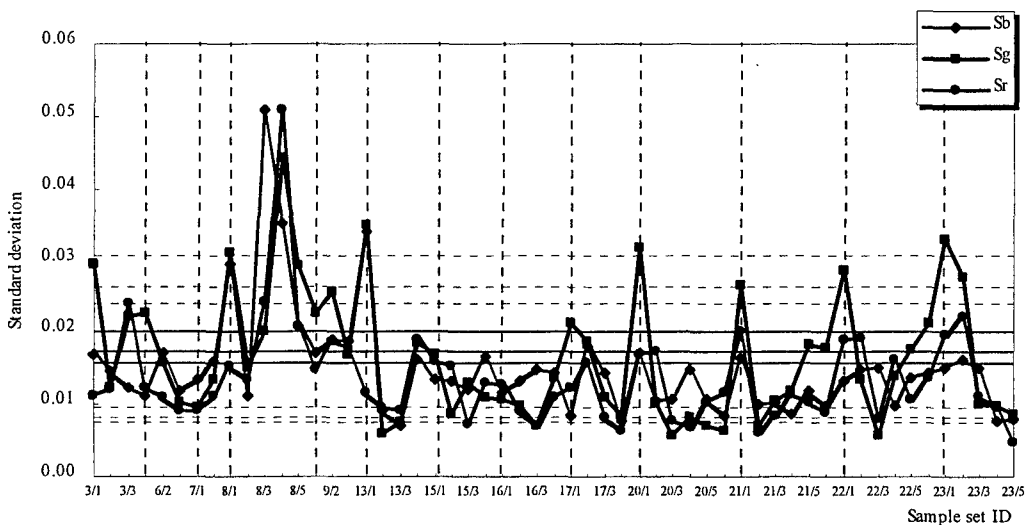


Figure 9. Control chart for standard deviations, S's, with 3-sigma control limits for 13 running days

5. RESULTS AND DISCUSSIONS

5.1. Verification of DSLI

Figure 10 summarizes the overall delta E_{ab}^* of each patch of two central mockups in the initial stage and the third DSLI stage. During performing DSLI three times, the interval settings of DSLI, that are the size of subgroup, were 8, 4 and 2, respectively. Results showed that DSLI could improve the color accuracy of all patches. However, there were some patches did not act as well as the overwhelming majority of patches. For example, the values of delta E_{ab}^* of C7, G7, G8, H7, K4 and L4 patch were over 6. One interesting phenomenon was that all these abnormal patches were close to high chroma. In other words, the usability of DSLI was limited to these color patches in this study. This phenomenon will be investigated in the following solution. DSLI did not consider that chroma information at the same level of hue and lightness. For abnormal patches, we adopted other accuracy patches, which were at the same level of hue and lightness in the final stage. For instance, we use polynomial curve fitting function to fit C5, C6 and C8 in RGB mode and evaluate the polynomial at C7. In general, only one color channel needs processing.

Figure 11 shows averages and maximums of delta E_{ab}^* resulting from the initial stage to the final stage. The average of delta E_{ab}^* was 9.01 and the standard deviation of delta E_{ab}^* was 5.51 in the initial stage, which did not employ DSLI. Through using DSLI once, the average of delta E_{ab}^* was 3.73 and the standard deviation of delta E_{ab}^* was 3.21, and so on. After performing DSLI three times, we called the third DSLI stage, the average of delta E_{ab}^* was downward to 1.69 and the standard deviation of delta E_{ab}^* was also downward to 1.46. These results are listed in Table 2.

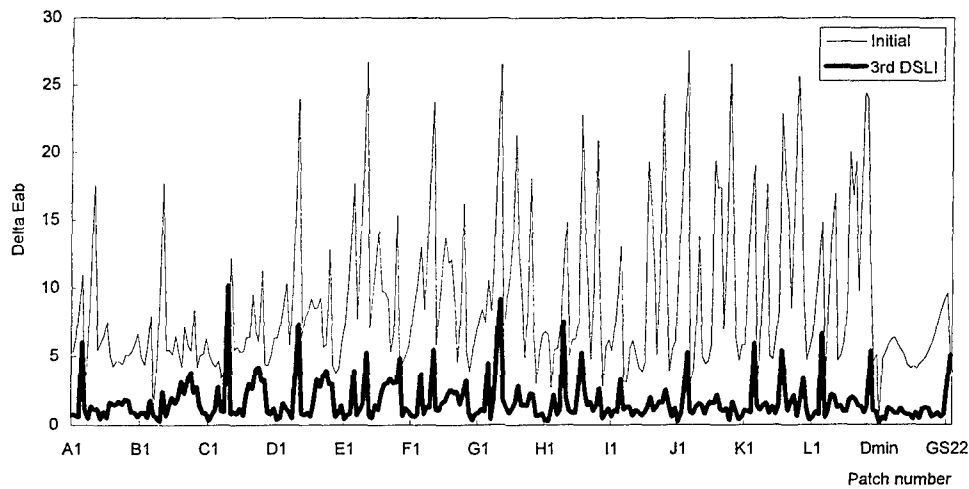


Figure 10. Comparisons of the distributions of delta E_{ab}^* of the central mockup between the initial and third stages

Table 2. Statistic analysis results form the initial stage to the final stage

| delta E_{ab}^* | Initial stage | 1st DSLI stage | 2nd DSLI stage | 3rd DSLI stage | Final non-DSLI stage |
|--------------------|---------------|----------------|----------------|----------------|----------------------|
| Maximum | 27.58 | 19.53 | 14.00 | 10.18 | 6.66 |
| Minimum | 0.33 | 0.22 | 0.24 | 0.16 | 0.05 |
| Average | 9.01 | 3.73 | 2.35 | 1.69 | 1.554 |
| Standard deviation | 5.51 | 3.21 | 1.73 | 1.46 | 1.31 |

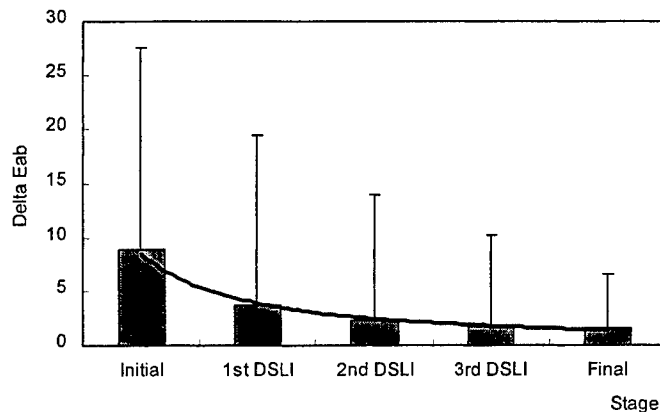


Figure 11. Efficiency of implementing DSLI in decreasing the average and the maximum of delta Eab*

5.2. Long-term testing

For long-term testing the production process, in this experiment, we randomly sampled one target and measured it from 20 produced calibration targets per workday. The measurement conditions were likely to 4.1. The average and the standard deviation of delta Eab* for one sample were computed. Averages and standard deviations of delta Eab* from 20 samples are collected, as shown in Figure 12. Results demonstrated that we could control averages of delta Eab* between 1.48 and 1.96 and standard deviations between 1.62 and 1.06 (Figure 12 (a)). The overall average of delta Eab* was 1.72 and the average of standard deviations of delta Eab* was 1.34 (Figure 12 (b)). A value of 1.34 means that 99% of the calibration targets will be with a delta Eab* of 4.489 (3.35× average of standard deviation) of the manufacturing aim values.¹³ During the long-term testing, the fluctuations of average delta Eab* became larger day by day. As Figure 12 (b) depicts, standard deviations were over the average of over all standard deviations in a later period. Theoretically, if manufacturing process happens to be out of control, DLSI is still practical.

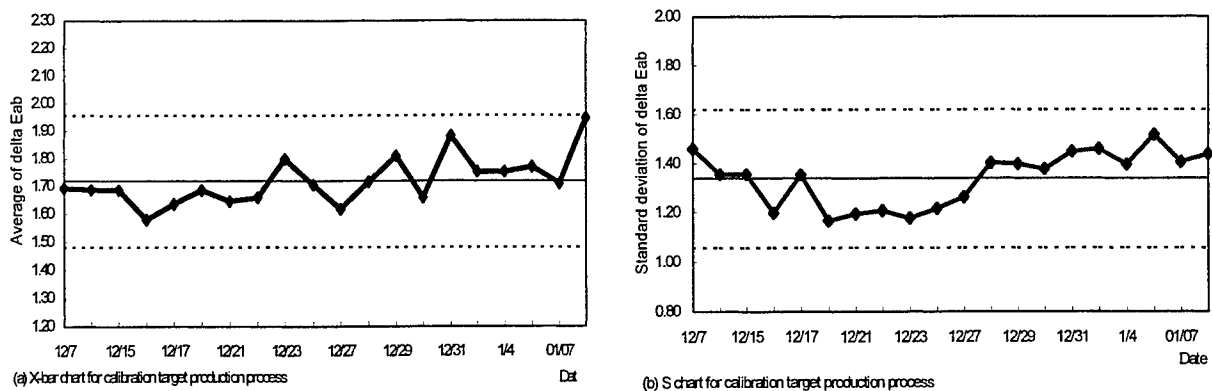


Figure 12. X-bar and S chart for calibration target production process

6. CONCLUSION

This paper has discussed how to design and produce the calibration targets for digital input color devices. In addition, this study has thoroughly examined the effectiveness of DSLI and has capably controlled the quality of calibration targets from a field experiment. We infer that the approach is also suitable for manufacturing transparent targets. Up to present, although

some researches have focused on development of virtual spectral color target, there are still some limitations, such as metamerism.¹³ Real color patches, made of photographic materials, have smoother spectral shapes than the virtual color patches. However, because this study has specified some self-determinations differ with ISO 12641, the feasibility of the calibration target will be compared with other vendors in future works.

REFERENCE

1. Tony Johnson, "Methods for characterizing colour scanners and digital cameras," *Displays*, **6(4)**, pp.183-191 (1996).
2. ISO, *ISO/FDIS 12641 Graphic Technology—Prepress Digital Data Exchange—Colour Targets for Input Scanner Calibration*, 1997.
3. T. G. Maier and C. E. Rinehart, "Design Criteria for an Input Color Scanner Evaluation Test Object," *TAGA Proceedings*, pp. 469-483, 1988,
4. ANSI, *ANSI IT8.7/2-1993 Graphic technology—Color reflection target for input scanner calibration*.
5. H. R. Kang, "Color scanner calibration of reflected samples," *SPIE Vol. 1670 Color Hard Copy and Graphic Arts*, pp. 468-477, 1992.
6. Ohta, N., "The Color Gamut Obtainable by the Combination of Subtractive Color Dyes. V. Optimum Absorption Bands as Defined by Nonlinear Optimization Technique." *Journal of Imaging Science*, **30(1)**, pp. 9-12, 1986.
7. Inui, M., "A Fast Algorithm for Computing the Colour Gamut of Subtractive Colour Mixture." *Journal of Photographic Science*, **38(4,5)**, pp. 163-164, 1990.
8. CIE 15.2, *Colorimetry*, Second edition, 1986.
9. M. Stokes, M. Anderson, S. Chandrasekar and R. Motta, "A standard default color space for the Internet – sRGB," Version 1.10, <http://www.w3.org/Graphics/Color/SRGB.html>, 1996.
10. M. Nielsen and M. Stokes, "The Creation of the sRGB ICC profile," *Proceedings of IS&T/SID 1999 Color Imaging Conference: Color, Systems, and Applications*, pp. 253-257, 1999.
11. J. M. Kasson, "Performing color space conversions with three-dimension linear interpolation," *Journal of Electronic Imaging*, **4(3)**, pp. 226-250, 1995.
12. W. J. Kolarik, *Creating Quality: Concepts, Systems, Strategies, and Tools*, McGraw-Hill, New York, 1995.
13. F. K. Dolezalek, "Appraisal of production run fluctuations from color measurements in the image," *TAGA Proceedings*, pp. 154-164, 1994.
14. H. Kotera, H. S. Chen and R. Saito, "Generation of virtual spectral target and its applications," *Proceedings of The Seventh IS&T/SID Color Image Conference: Color Science, Systems and Applications*, pp. 36-41, November 16-19, Scottsdale, Arizona, USA, 1999.